Research Article ISSN 2250-0480 VOL 6/ ISSUE 4/OCTOBER 2016

International Journal of
Life science & Pharma Research

INVESTIGATING VARIOUS FACTORS TO INCREASE THE STRENGTH OF ALUMINA NANO-FIBERS USING SOL-GEL METHOD

*ALIREZA SAMADI TABRIZI

Department of Materials Engineering,
Science and Research Branch,
Islamic Azad University, Tehran, Iran

ABSTRACT

Aluminum fibers are important due to their high strength and resistance against metals and non-oxide materials slag, chemical stability up to 1000, low heat generation, and appropriate electrical cinsulation. The most important alumina fibers are used as metal or ceramic reinforcement and cause the improvement of physical and mechanical properties. Therefore, it is necessary to provide high strength fiber with appropriate shape. The purpose of the present study is to add these materials and reach the best fibers in terms of shape, strength and diameter through sol-gel method. Hence, we attempt to investigate various factors effect and obtain strong fibers using sol-gel method.

KEYWORDS: *Alumina fiber, sol-gel method, nano-fiber*

INTRODUCTION

In sol-gel method, sol is hydrolyzed till an appropriate viscosity is obtained to produce fiber. Alumina fibers are regarded as a very important engineering finding. These fibers have many applications such as catalyst base in high-temperature reactions, fire protection and resins, metal and ceramic reinforcement [1]. Aluminum fibers are important due to their high strength and resistance against metals and non-oxide materials slag, chemical stability up to 1000°C, low heat generation, and appropriate electrical cinsulation. The most important alumina fibers are used as metal or ceramic reinforcement and cause the improvement of physical and mechanical properties. Therefore, it is necessary to provide high strength fiber with appropriate shape [2]. As an important problem in providing fibers, we can refer to the problem of sticking fibers with different diameters to each other, creating hollow fibers, fibers cracking, heavy production cost, and strength decrease in high temperature (1000°C) and in rust-susceptible humid air [3]. One of the most effective methods of ceramic fiber production is sol-gel technique. The main advantages of sol-gel method, compared to other conventional methods, is its mechanism in low temperature, products homogeneity, fibers' uniform diameters, similar shape, and appropriate control of fibers' final features. To improve flaws of fibers, sol spinning features including viscosity and polymer building spinning sol should be investigated.Spinning soles should be polymer linear shape and show Newton behavior; i.e., viscosity should be independent of cut speed to produce sequential fibers. Regarding sols with non-Newton viscosity, 3D polymer building occurs. This feature of sol is not appropriate for fiber production. Viscosity in sol spinning is another important feature which should be properly controlled. For the study, fibers which were produced from sol had a viscosity bout 100P. Desirable viscosity for sol should be as much as it produces fibers during spinning process. During spinning process, a low-viscosity sol causes the formation of some drops while, a high-viscosity sol causes to the rapid creation of gel. Adding appropriate spinning such as 0.1% to 10% of PVA, PEG, Lactic acid, PVP, and PED weight to the gel, gel formation can be avoided somehow. However, to prepare desirable fiber, organic amount should be minimized to decrease volatility at calcinations stage. Further, alumina alpha is formed at a temperature higher than 1000 °C which leads to rapid growth of grains and decreasing fibers' strength. To improve mechanical properties, some additives such as M_gO, SiO_2 and Fe_2O_3 control this issue and enhance mechanical strength [4]. Many studies have been conducted on increasing alumina strength [5-11]. The present study is an attempt to investigate various factors to increase the strength of aluminanano-fibers using sol-gel method. Aluminanano-fiber with the least diameter without adherence is synthesized through sol-gel method. Hence, there is a need of investigating various factors to increase the strength of aluminanano-fibers using sol-gel method. Obtaining its optimum amount through sol-gel method can be regarded as the innovative aspect of this research.

RELATED LITRATURE

Surface modification causes to improving corrosion, increasing corrosion resistance, decreasing ion release, and improving biocompatibility [13]. Various modification methods such as PVD and Andonizing [14], sol-gel [15] and Electrophoresis [16] have been employed to improve corrosion resistance and alumina biocompatibility. One of the most important coating parameters is to use appropriate method to create coating with appropriate density, uniformity and cohesion [17]. Electrolytic Plasma Process (EPP) method can be also employed as a technique to create ceramic coating on metals. As the previously conducted studies reported, the coatings created in this way cause to create a high corrosion resistance and anti-corrosion characteristics in the surface of metal [8]. This method significantly increases surface properties of metals such as oxidation resistance, corrosion resistance, and intra-surface association [19]. So far, many coatings have been created using this method. For example, we can refer to the study performed by Kern et al. using EPP method [19]. In another study, alumina silica composite has been coated for plan applications [12]. Due to a combination of high corrosion resistance, good biocompatibility, and high strength, $Al_2O_3$is used [20]. Various ceramic coats such as Zirconia [15] and Hydroxyapatite [21] have been applied on stainless L316 metal by different methods. Barik et al. (2005) applied Al_2O_3 coating using plasma electrolyticoxidation method and investigated it s corrosion properties on aluminum alloy 6082 [22]. Sarafoglou et al. (2007) explored Al_2O_3coating on AISI 316 stainless using controlled atmosphericplasma spray[23].In another electrochemical study, corrosion resistance behavior of Hydroxyapatite on stainless metal created by EPD method was analyzed [24]. Other researchers in 2013 improved Hydroxyapatite coatings properties created by plasma coating through reinforcing Al_2O_3particles [25].

METHOD

For sol-gel mechanism, precursor is of alumina fiber including Oxy-aluminum chloride, base aluminum chloride, curling irons, aluminum acetate, and andaluminumacetatemonohydrate. asically, sol-gel mechanism of aluminum fibers has the following stages: Preparing sol by permitted additives and achieving an appropriate rheology for spinning, liquid spinning to achieve gel fibers, and gel fivers calcinations to obtain final oxide fibers. It is highly important to well control all the above three stages to obtain high-quality fibers with final desirable features. For preparation, alumina sols should be prepared through detailed changes in the known Oxychloridemethod. With silica additives as sintering assistant and Lactic acid as spinning assistant, sol was spine through a home spinner with 120 0.4 mm-diameter holes and speed of 2000 rpm. The spine fibers were collected in a mat-like cylinder. The fibers were heated at a temperature of 60°Cwith a relative humidity of 50% to prevent sticking to each other. The fibers dried by fibers were calcinated with different scheduling in different temperatures (up to 1400°C) to produce silica alumina fibers (weight of 4%). Using electronic microscopic scanning, micro-structural related features were investigated and observed. The viscosity of gel was measured by Kaake VT550. Further, the mentioned additives (such as glue and spinning assistance) were added and their effect was analyzed. Finally, FTIR, TEM and XRD analyses were performed [3]. To produce 1-D alumina, aluminum II with high purity and Pentane Dion IIII [$Al(CH_3COCHCOCH_3)_3$] with the purity of 99.995% were employed in alumina fibers synthesis process. Adequate amount of clear white powder is solved by mildly shaking in ACS and acetone grading to gain a clear liquid. The saturation of AP liquid which is used in this work is 0.85×10^{-2}mol L^{-1}. Polyvinylpyrrolidoneis used in polymer element of all combinations. This polymer liquid is subjected to intense shake by solving PVP powder in ethanol reagent to gain 15%wt. of PVP liquid. This saturation was performed. After several primary reiterations, desirable viscosity was selected in organic and non-organic liquids combinations. In electro-spinning experiments, the average amount of precursor liquids (AP and PVP) was added to beaker and combined through magnetic stirrer to form cohesive and homogeneous liquid. After combining, this liquid was floated in Benton-Dickinsom medical syringe (with the capacity of 5ml). Figure 1 shows collector template design [6-8]. To prepare porous and coated alumina, pre-structural sub-layers of Au should be produced from porous alumina frames (Al_2O_3). Anodizing high-porosity aluminum foil coating (99.99%) is continued under constant voltage (4W) in Oxalic acid solution (duration of first and second anodizationhas been 8 hours and 1 hour, respectively). Apertures produced in this process had a diameter of about 40 nm and center-to-center distance of 105 nm. Passing this process, a thin layer of Au was changed into a thick deposit on the frames (Emitech-K550). Using 12 w DC power for Au layer, the distance between sub-layer became 2.5 cm. the thickness of Au layer was changed by changing deposit time between 0-10 minutes [30]. To make clear alumina nano-fibers through electro-spinning, just like making nano-fibers in 1D section, PVP liquid was made by solving PVP powder in ethanol reagent through intensely and constantly shaking. Aluminum precursor liquid remained clear in acetone and it did not require any retrofitting during long time without any golden substance. Equal to the amount of precursor liquids for electro-spinning experiments (PVP and AP), after injecting the combination in Benton-Dickson medical syringe (5ml), it was completely mixed in homogeneous cohesive liquid [34]. To prepare spine alumina fiber, alumina gels should be prepared by creating the least changes in known oxycholoride method. Aluminum oxychloride sols that 30.5% of its weight was formed by alumina were prepared. These sols had a viscosity of 5P. These sols, then, were combined with SiO_2 and Lactic acid or PAV with Stoichiometric ratio. Afterwards, they were heated at the temperature of 70 °Cwith a viscosity about 100P. Finally, they were spine by spinerette. This spinerette had 120 0.4mm-diameter holes which rotated with the speed of 2000rpm. The spine fibers were collected in a mat-like cylinder. The fibers were heated at a temperature of 60°C with a relative humidity of 50% to prevent sticking to each other. The fibers dried by fibers were calcinated with different scheduling in different temperatures of 500, 950 and 1200 °C [36-37]. To prepare alumina sol in triple combination, $MgNO_3$ should be added to the sol such that the final combination contains 1 and 2% MgO. Hydroxyethyl cellulose (HEC) was added to the sol as cohesive to obtain a balanced strength and flexibility. Then, removing water, the sol became thick to reach the required solid volume. When the sol became appropriate to form fibers, 10ml syringe was added and fibers were stretched in a triangular crystal container containing ammonia liquid. Next, the in-gel fibers were separated from ammonia liquid and dried at the room temperature. The dried fibers were sintered for 2 hours at the temperature of 1600 °C with heating speed of 5°C in minute [39-4].

RESULTS

The Effect of Temperature

Figure 1 shows gel and powder X-ray design in various temperatures. As shown in the figure, at the temperature of 500°C, the gel is totally amorphous. The gel, in fact, has been formed at low temperatures from aluminum hydroxide groups which are analyzed by increasing the temperature of hydroxide groups. At the temperature of 900 °C, alumina phase of X with a cubic structure is formed. As a result of increasing the temperature up to 1000 °C, alumina phase of X is changed into KAPPA alumina. Simultaneously, alpha alumina phase peaks are emerged and the peaks intensity is increased by increasing the temperature such that alpha phase totally becomes stable at the temperature of 1100°Cand the middle phases are disappeared. As shown in the figure, the gel's weight is decreased up to 50% at the temperature of 700 °Csuch that the weight reduction at 300°C pertains to water exit and heating peak in this temperature also pertains to this phenomenon. At this stage, weight reduction is about 35%. Between 300 to 600 °C, the weight reduction level is increased (about 5%) and volatiles exit is not considerable. Increasing temperature to 600 °C led to higher weight reduction due to exiting chlorine from the gel. Increasing temperature from 75°C led to no reduction in weight and all volatiles exist from the gel and form middle phases of alumina and phase changes begin at higher temperatures. Figure 2 shows scanning electron microscope images from alumina powder. These powders have been calcinated at 1100 °C for 3 hours. As shown in the figure, the size of grains is 200 nm on average and the smallest grain has a size of 32 nm. Figures 3 and 4 pertain to TEM images from calcinated species at the temperatures of 1100 and 1200 °C. According to the figures, considerable amounts of particles are below 100 nm. In higher magnifications, crystallization can be clearly seen. Testing temperature revealed that at low temperatures, the gel is amorphous while at high temperatures, alumina middle phases are appeared and these phases are changed into alpha alumina. Increasing the temperatures, the gel firstly loses its water at the temperature of 300°Cand chlorine existing in the gel exits at the temperature of 700 °C. Alpha alumina powder produced in this way has a size of 200 nm and the smallest particles reaches 32 nm.

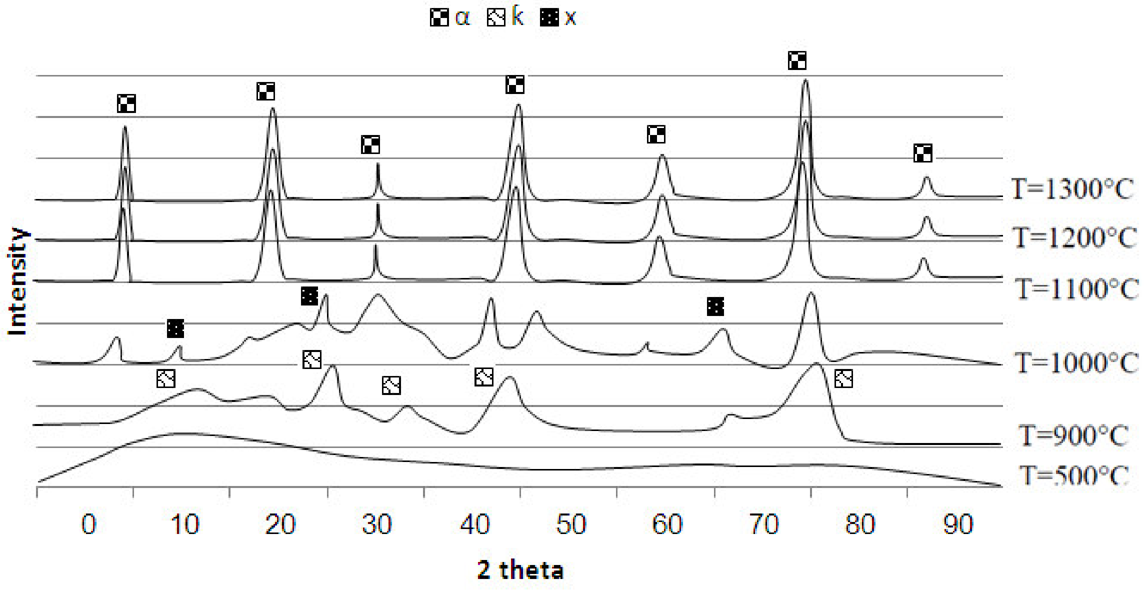

Figure 1
XRD pattern for temperature changes

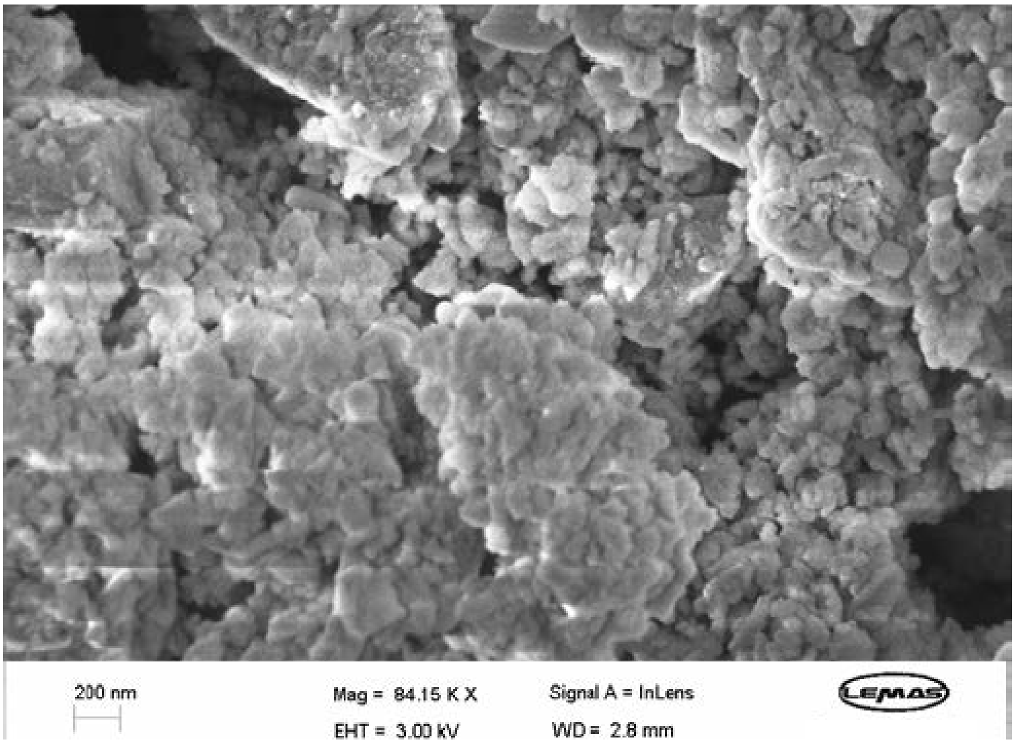

Figure 2
Alpha alumina powder calcinated at 1200 ℃

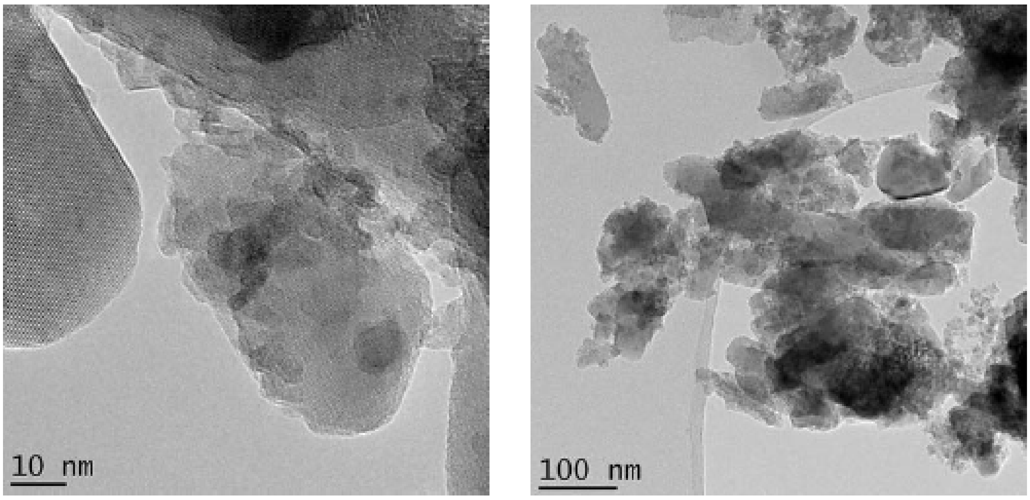

Figure 3
Calcinated species at 1100℃ in two different magnifications

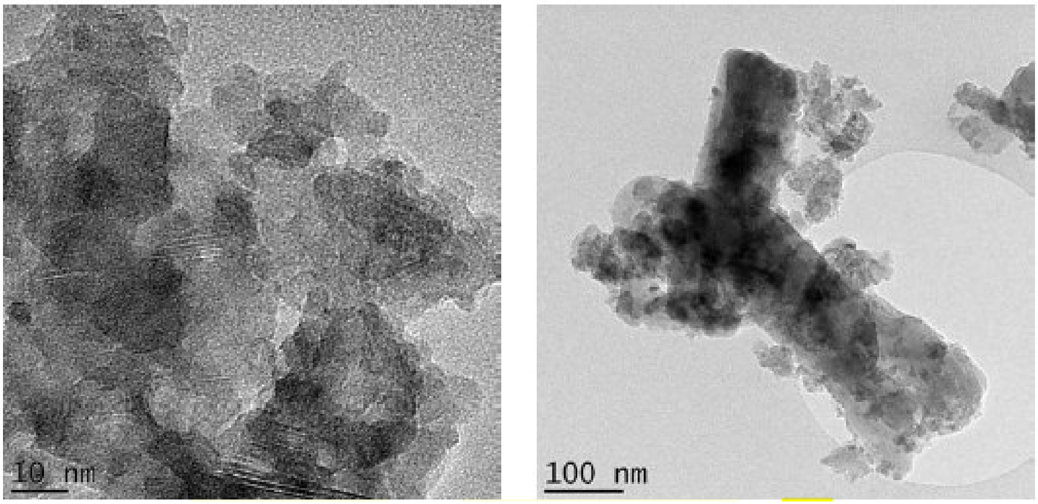

Figure 4.
Calcinated species at 1200℃ in two different magnifications

Accumulation

Extraordinary absorption capacity indicates high amount of aperture in species which are prepared with PEO. Porosity level is attributed to empty inter-crystal spaces in accumulated nano fibers of alumina. The important feature of nano fibers structure is their high resistance at high temperature. BET specific surface area information and species' porosity at three temperatures shown in Figure 5 are purified. For the species prepared by PEO active materials, downhill increase in desorption, from 1 P/P_0 about 0.7, refers to high level of porosity while desorption capacity b (w/o PEO) is low for the species.

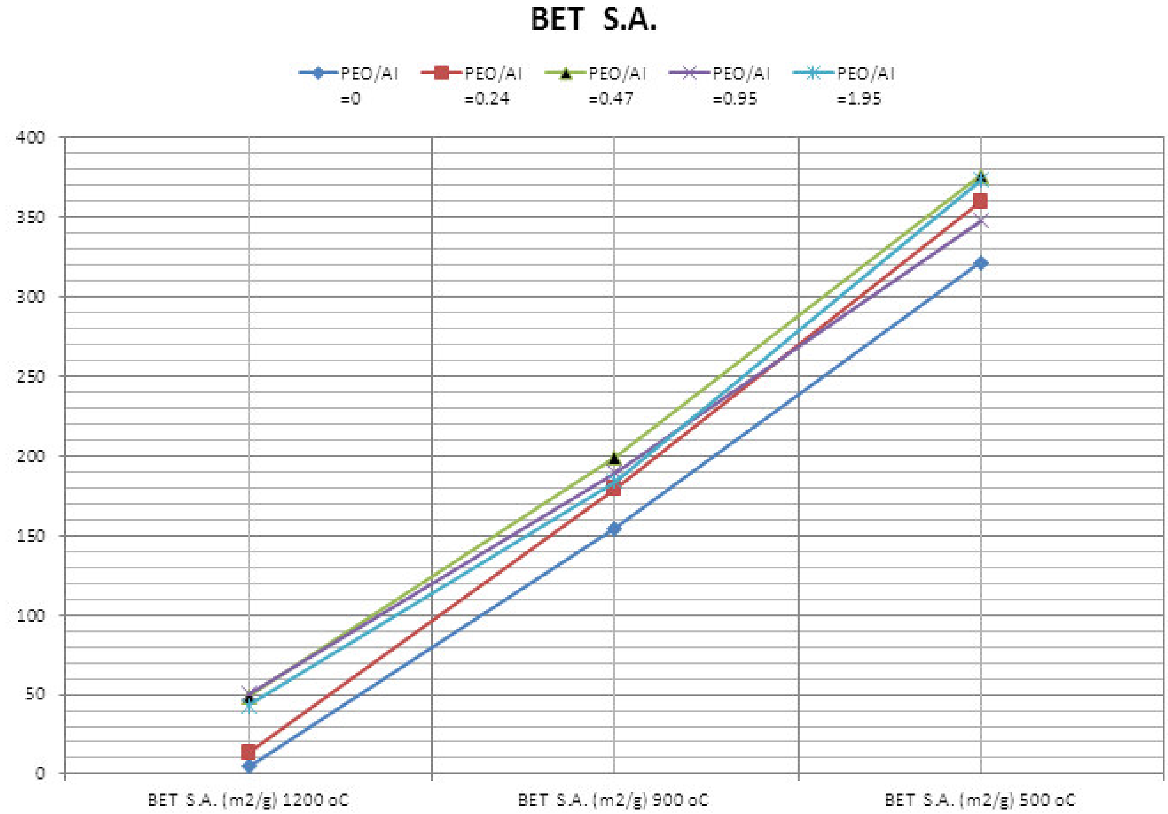

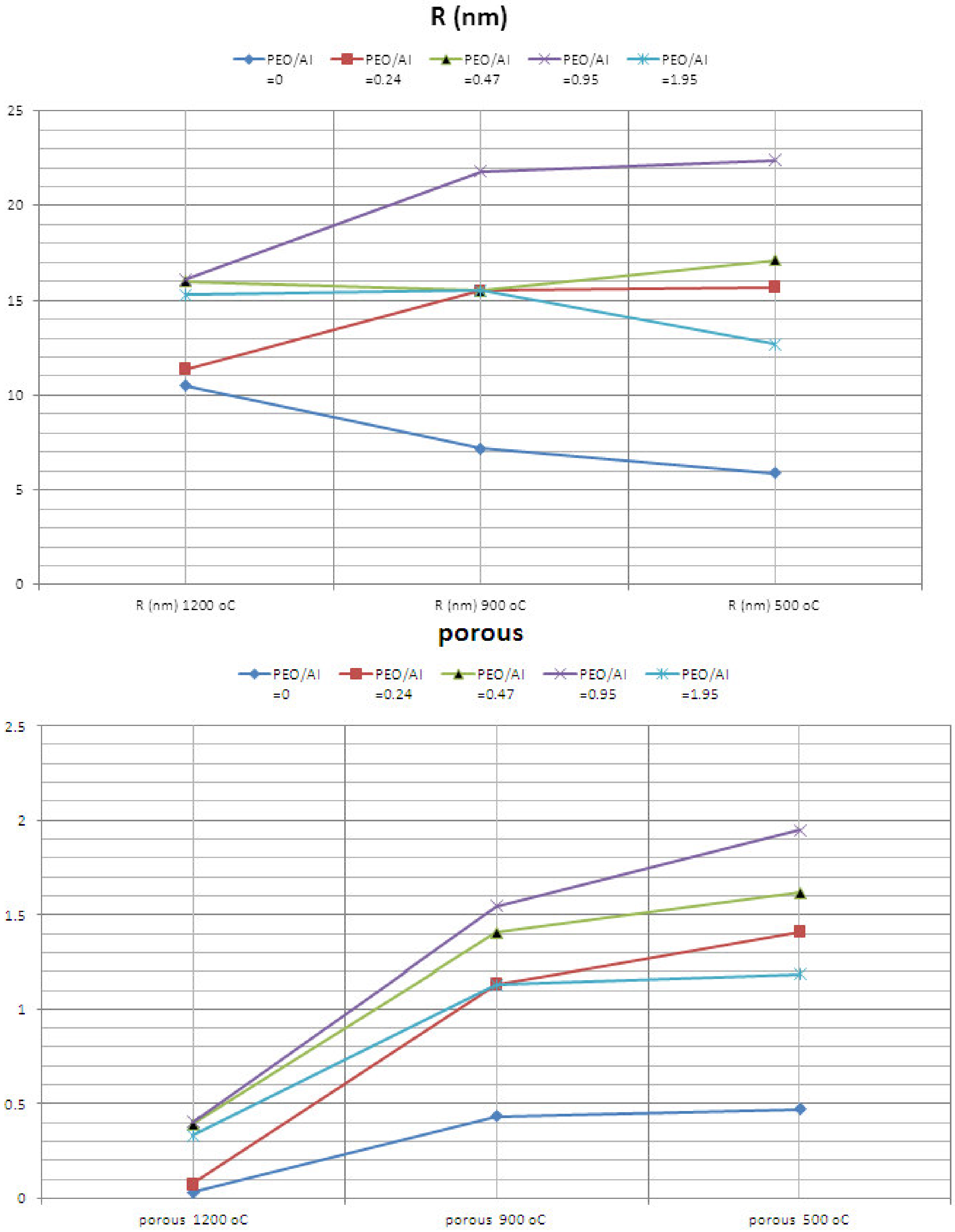

Figure 5
Accumulation

Random accumulation of alumina nano fibers leads to highly porous texture. Obviously, superficial nitrogen absorption depends on its porosity. Alumina prepared without nitrogen absorbs more than 300 cm3/g STP and PEO in 77k. While, this prepared species absorbs 1050 cm^3/g STP at the presence of PEO. At liquid state, the chains of PEO active materials tend to accumulation close to each other and oxide groups are created by forming ravine. When active substance is scattered in the middle of pole like watery systems or polar surfaces, oxide groups, external surface of ravines at the presence of contact with the middle of pole and Bohemia crystal surface will be formed. Change in peak failure from lower angle indicates the interaction between active materials' oxide groups and Bohemia crystallites surface. This hydrogen association does not seem adequately strong against natural changes in Bohemia crystallites; but, it may lead to oxide groups' accumulation in active materials. It is due to the fact that active materials molecules accumulation has higher flexibility.

Electric Field

Figure 6 shows microscopic images of spine fibers. Unique fibers with uniform features and relatively high slope are easily seen. Direct tendency to spine fibers under the impact of pressure imposed on electric field is obvious. SEM images in fibers combination burning in constant pressure of air at the temperature of 1300 ℃ have been also presented. As observed, the main characteristics which are obtained in spines combination are totally maintained in burned species while predicting considerable decrease in fibers' diameter. As shown in Figure 7, DES fiber of Al_2O_3 which were burned at 1500 ℃ for 1hour revealed that increasing calcinations temperature leads to the clarity of particles; association, inter-particle conductivity and inter-fiber connection. As Figure 7 shows, dispersive spectrum of ED's energy in alumina fibers burning for 1 hour at 1000 and 1500 ℃ are obtained. These spectrums refer to the presence of aluminum and oxygen separately. After this heating behavior, Al_2O_3 is obtained.

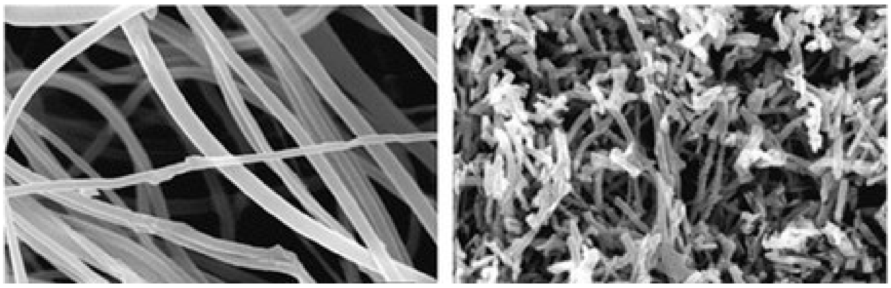

Figure 6
Microscopic image of spine fibers of AP-PVP

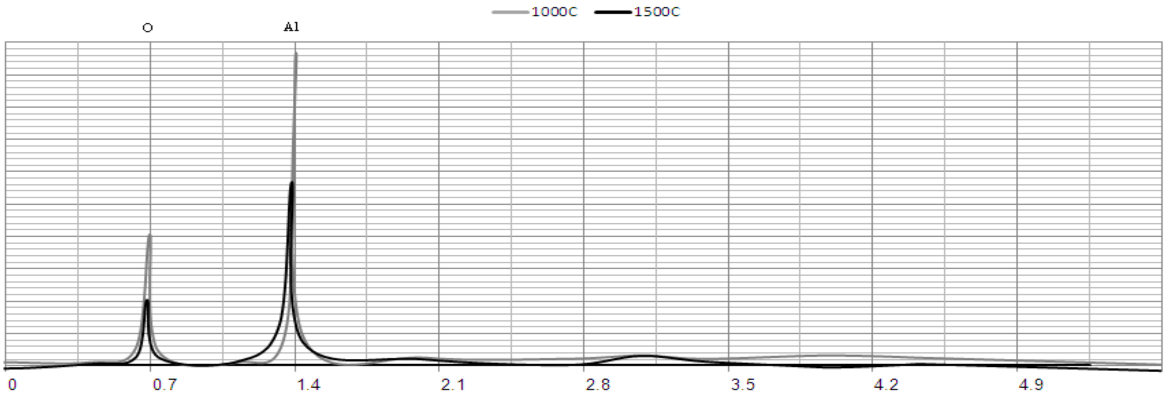

Figure 7
EDS image pertained to 1000 and 1500℃

Electrospinning

SEM images of combination fibers burning at 1000 and 1300℃ are shown in Figure 8. As observed, fiber features are maintained in spine combination burning in species with a considerable decrease in fibers' diameter.

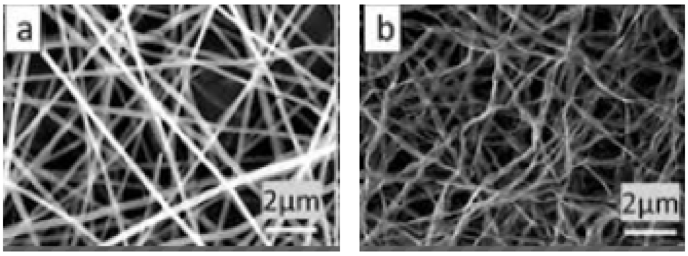

Figure 8
SEM images of vaccinated fibers: a) 1000℃, b) 1300℃ for 1 hour

EDS spectrum existing on fibers burning at 1000 ℃ for 1 hour has been shown in Figure 9 and indicates the presence of aluminum and oxygen. After burning fibers at 1500℃ for 1 hour, 56% aluminum is obtained in these fibers.

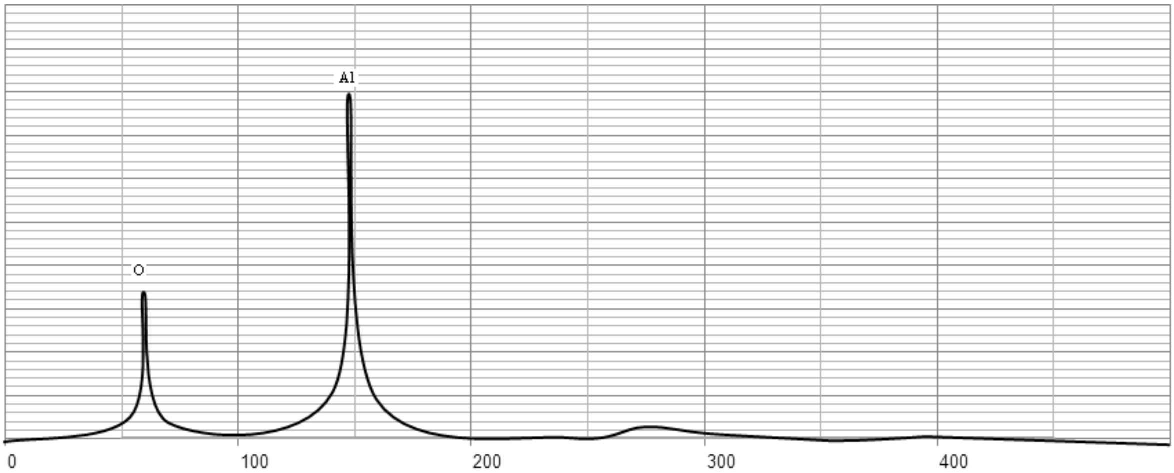

Figure 9
EDS sign in electrospine fibers burning at 1500℃

Combination

In Figure 10a, real images of sintered fibers, alumina-zirconium-magnezium,are presented. Micro-structures of alumina and alumina-zirconium are shown. When MgO content is increase about 2%, grain size is decreased. Grain size of alumina fiber without MgO varies from 1 to 4 μm. While 2% MgO changes this value from 1 to 2.07 μm. For alumina-zirconium fiber without MgO, grain size is 1-4 μm. When MgO is added up to 2%, grain size is changed from 1 to 3 μm. At the presence of MgO, the temperature of crystallization phase of**α**-$Al_2O_3$was 125 ℃. Increasing temperature is the result of increasing resistance to phase change with grain size reduction. Heating peak of 1290℃ in zirconium-alumina fiber without MgO is accompanied with**α**-Al_2O_3 crystallization. Aluminum hydroxide and its derivatives were dehydrated to create concentration state by changing aperture structure into changed alumina. A-alumina formation from the changed alumina includes ordering oxygen latticing from the changed cubes into a closed hexagonal structure. Probably, zirconium ions cause to create a force in aluminum ions dissemination. Therefore, transferring to **α**-Al_2O_3 at the presence of zirconium occurs at higher temperatures. When MgO content is increased up to 2%, temperature is increased up to 1320 ℃. The effect of MgO and ZrO_2 leads to the increase of change in temperature.The effect of MgO in alumina-zirconium fiber is less than alumina fiber due to the lack of solving MgO in zirconium.

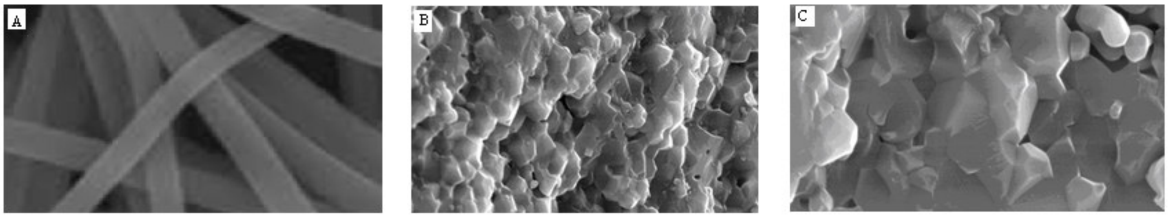

Figure 10
SEM images of combination

CONCLUSION

The purpose of the present study is to add these materials and reach the best fibers in terms of shape, strength and diameter through sol-gel method. Hence, we attempt to investigate various factors effect and obtain strong fibers using sol-gel method. This work proved that a-alumina fibers with uniform diameter, high structural quality and high slope ratio can be produced through electrospinning technique. We found out that there is the possibility of parahegsaphylnano fibers growth on porous nano alumina frames coated by high layering through physical stem deposit. The new proposed design of this work is useful for low temperature, aqua synthesis of oxides and other combinations as well as nano structural ceramics. **γ**-Al_2O_3 nano fibers provide with an opportunity to observe the effect and absorption with associating scientific groups on external fibers. It is due to the fact that they have superficial areas with large aperture and wider surface ratio. Octyle group associating with nano fibers indicates its highhydrophobicity. Using **γ**-Al_2O_3 nano fibers for easy access has been proved to be useful since it can influence specifying disseminated issuesand optimize absorbent and catalysts production with better function in future.

REFERENCES

1 AyadL.The extracellular matrix factsbook.New York, NY: *Plenum Press*; 1994.

2 Kaplan FS, Hayes WC, Keaveny TM, Boskey A, Einhorn TA, IannottiJP.Form and function of bone.In: Simon SP, editor. *Orthopedic basic science*.Columbu s, OH: American Academy of Orthopedic Surgeons; 1994.p.127–85.

3 Price RL, Gutwein LG, Kaledin L, Tepper F, Webster TJ. Osteoblast function on nanophase alumina materials: *influence of chemistry*, phase, and topography.J. Biomed Mater Res 2003; 67(4):1284–93.

4 T. Subbiah, G.S. Bhat, R.W. Tock, S. Parameswaran, and S.S. Ramkumar, “Electrospinning of nanofibers”, *J. Appl. Polymer Sci*. 96, 557–569 (2005).

5 S. A. Hassanzadeh-Tabrizi, E. Taheri-Nassaj, “Sol–gel synthesis and characterization of Al2O3–CeO2 composite nanopowder”, *J. Alloy. Compd*., Vol. 494, 2010, pp. 289-294.X

6 A. Sedaghat, E. Taheri-Nassaj, R.Naghizadeh, “An alumina mat with a nano microstructure prepared by centrifugal spinning method”, *J. Non-Cryst. Solids*, Vol. 352, 2006, pp. 2818-2828.X

7 Wierzbicki TA, Lee IC, Gupta AK. Combustion of propane with Pt and Rh catalysts in a meso-scale heat recirculating combustor. Appl Energy 2014;130:350–6.X

8 A.L. Ahmad, N.N.N. Mustafa, *International Journal of HydrogenEnergy* 32, 2010, 2010–2021.

9 I. Gandarias, P.L. Arias, J. Requies, M. El Doukkali, M.B. Güemez, *Journal of Catalysis* 282, 2011, 237–247.

10 A. Iriondo, J.F. Cambra, V.L. Barrio, M.B. Guemez, P.L. Arias, M.C. Sanchez-Sanchez, R.M. Navarro,

11 J.L.G. Fierro, *Applied CatalysisB: Environmental* 106, 201, 83–93.

12 M. El Doukkali, A. Iriondo, P.L. Arias, J.F. Cambra, I. Gandrias, V.L. Barrio, *International Journal of Hydrogen Energy* 37 (2012) 8298–8309.

13 S.K. Tiwari, T. Mishra, M.K. Gunjan, A.S. Bhattacharyya, T.B. Singh, and R. Singh "Development and Characterization of Sol-Gel Silica-Alumina Composite Coatings on AISI 316L for Implant Applications", *Surface & Coatings Technology*, Vol. 201, pp. 7582-7588, 2007.

14 S. Nagarajan, N. Rajendran "Sol-Gel Derived Porous Zirconum Dioxide Coated on 316L SS for Orthopedic applications", *J Sol-Gel SciTechnol*, Vol. 52, pp. 188-196, 2009.

15 W. Zhen-Jun, H. Li-ping, Ch. Zong-zhang, "Fabrication and Characterization of Hydroxyapatite/AL2O3 Biocomposite Coating on Titanium", *Trans Nonferrous Met. Soc. China*, 16, pp. 259-266, 2006.

16 Balmorgan, G. Balossier, S. Kannan, J. Michekl, J. Faure, S. Rajeswari, "Electro- chemical and Structural Characterization of Zirconia Reinforce Hydroxyapatite Bio- ceramic Sol-Gel Coatings on Surgical Grade 316L SS for Biomedical Applications", *Ceramic International*, Vol. 33, pp. 605-614, 2006.

17 Zh.Ch. Wang, Y.J.C. Huang, "Fabrication and Characterization of HAp/Al2O3 Composite Coating on Titanium Substrate", *J. Bio-medical Science and Engineering*, Vol. 1, pp. 190-194, 2008.

18 P. Gupta, G. Tenhundfeld, E.O. Daigle, D. Ryabkov, "Electrolytic Plasma Technology: Science and Engineering- an Overview", *Surface & Coatings Technology*, Vol. 201, pp. 8746-8760, 2007.

19 Zh. Yao, Y. Jiang, Zh. Jiang, F. Wang, Zh. Wu, "Prepration and Structure of Ceramic Coatings Containing Zirconium Oxide on Ti Alloy by Plasma Electrolytic Oxidation", *Jornal of Materials Processing Technology*, Vol. 205, pp. 303-307, 2008.

20 P. Kern, P. Schwaller, J. Michler, "Electrolytic Deposition of Titania Films as Interface Coatings on Biomedical Implants: Microstructure, Chemistry and Nano-Mechanical Properties", *Thin Solid Film*s, Vol. 494, pp. 279-286, 2006.

21 N. R. Patel, P. P. Gohil, "A Review on Biomaterials: Scope, Applications & Human Anatomy Significance", *International Jornal of Emerging Technology and Advanced Engineering*, Vol. 2, Issue 4, 2012.

22 D.T.M. Thanh, Ph. T. Nam, N. T. Phuong, L. X. Que, N. V. Anh, Th. Hoang, T. D. Lam, "Controlling the Electrodeposition,Morphology and Structure of Hydroxy- apatite Coating on 316L Stainless Steel" *Materials Science and Engineering C*, Vol. 33, pp. 2037-2045, 2013.

23 R. C. Barik, J. A. Wharton, R. J. K. Wood, K. R. Stokes, R. L. Jones, "Corrosion, Erosion and Erosion-Corrosion Performance of Plasma Electrolytic Oxidation (PEO) Depositon Al2O3 Coatings", *Surface & Coating Technology*, Vol. 199, pp. s158-s167, 2005.

24 Ch. I. Sarafoglou, D. I. Pantelis, S. Beauvais, M. Jeandin, "Study of Al2O3 Coatings on AISI 316 Stainless Steel Obtained by Controlled Atmosphere Plasma Spraying (CAPS)", *Surface & Coating Technology*, Vol. 202, pp. 155-161, 2007.

25 K. Kh. Chew, Sh. H. Sh. Zein, A. L. Ahmad, D. S. Mcphail, M. F. Abdullah, "The Electrochemical Studies of the Corrosion Resistance Behavior of Hydroxyapatite Coatings on Stainless Steel Fabricated by Electrophoretic Deposition", *Jornal of Industrial and Engineering Chemistry*, Vol. 19, pp. 1123-1129, 2013.

26 M. Mittal, S.K. Nath, S. Prakash, "Improvement in Mechanical Properties of Plasma Spray Hydroxyapatite Coatings by Al2O3 Reinforcment", *Material Science and Engineering C*, Vol. C 33, pp. 2838-2845, 2013.

27 T. Subbiah, G.S. Bhat, R.W. Tock, S. Parameswaran, and S.S. Ramkumar, "Electrospinning of nanofibers", *J. Appl. Polymer Sci. 96, 557–569* (2005).

28 I. Chun, Fine Fibers Spun by Electrospinning Process from Polymer Solutions and Polymer Melts, Ph.D. Dissertation, *University of Akron*, 1995.

29 D.H. Reneker, A.L. Yarin, H. Fong, and S. Koomhongse, "Bending instability of electrically charged liquid jets of polymer solutions in

electrospinning", *J. Appl. Phys*. 87, 4531–4547 (2000).

30 G. Koller, S. Berkebile, J.R. Krenn, G. Tzvetkov, G. Hlawacek, O. Lengyel, F. Netzer, C. Teichert, R. Resel, M.G. Ramsey, *Adv. Mater*. 16, 2159 (2004)

31 F. Balzer, L. Kankate, H. Niehus, R. Frese, C. Maibohm, H.-G. Rubahn, *Nanotechnolog*y 17, 984 (2006)

32 S. Müllegger, G. Hlawacek, T. Haber, P. Frank, C. Teichert, R. Resel, A. Winkler, *Appl. Phys*. A 87, 103 (2007)

33 K.N. Baker, A.V. Fratini, T. Resch, H.C. Knachel, W.W. Adams, E.P. Socci, B.L. Farmer, *Polymer* 34, 1571 (1993)

34 F.W.C. Boswell, Proc. Phys. Soc. (London) A64 (1951) 465–478.

35 B.D. Cullity, Elements of X-ray Diffraction, 2nd ed., *Addison–Wesley, Reading*, MA, 1978.

36 K. Ishikawa, K. Yoshikawa, N. Okada, *Phys. Rev*. B 37 (1988) 5852–5855.

37 F. Zhang, S.W. Chan, J.E. Spanier, E. Apak, Q. Jin, R.D. Robinson, I.P. Herman, *Appl. Phys. Lett*. 80 (2002) 127–129.

38 Sopicka-Lijer, M., Euro Ceramics, Vol. 1, *Elsevier Applied Science, New York,* 1989, 1609±1612.

39 Sato, T., Ikoma, S. and Ogana, K., Thermal Analysis, Vol. 1, *Proceedings of the 7th International Conf. on Thermal Analysis*. John Wiley & Sons, New York, 1982, pp. 150±154.

40 Lewis, R. J. Sr., Hawleys Condensed Chemical Dictionary. *Van Nostrand, New York*, 1990.

41 Brinker, C. J. and Scherer, G. W., Sol±Gel science: The Physics and Chemistry of Sol±Gel Processing. *Academic Press, New York*, 1990, p. 295.